Example of a chaotic crystal: The labyrinth

M. Le Berre, E. Ressayre, and A. Tallet
Laboratoire de Photophysique Moléculaire, Bâtiment 210, Université de Paris–Sud, 91405 Orsay Cedex, France

Y. Pomeau
Laboratoire de Physique Statistique de l'ENS, 24 rue Lhomond, 75005 Paris Cedex 05, France

L. Di Menza
Laboratoire d'Analyse Numérique et EDP, Bâtiment 425, Université de Paris–Sud, 91405 Orsay Cedex, France
(Received 18 December 2001; revised manuscript received 12 April 2002; published 9 August 2002)

Labyrinthine structures often appear as the final steady state of pattern forming systems. Being disordered, they exhibit the same kind of short range positional order as the Newell-Pomeau turbulent crystal. Labyrinths can be seen as a limit case of the texture of disordered rolls with a coherence length of the same order as the wavelength. In the various two-dimensional model equations we looked at, labyrinths and parallel rolls are steady states for the same parameters, their occurrence depending on the initial conditions. Comparing the stability of these two structures, we find that in variational models their energy is very close, rolls always being more stable than labyrinths. For the nonvariational model we propose a numerical experiment which displays a well defined bifurcation from parallel rolls to labyrinths as the more stable state.

DOI: 10.1103/PhysRevE.66.026203 PACS number(s): 05.45.−a, 42.65.−k, 47.54.+r

I. INTRODUCTION

In nature, as in artificial systems, there is a wide variety of stationary patterns, from perfectly well ordered crystals or nonequilibrium patterns like Rayleigh-Bénard rolls and Bénard-Marangoni hexagons, to stationary ''chaotic'' structures without long range order like glasses for instance. The present paper is devoted to one particular instance of ''pattern forming'' equations that show both regular rolls and chaotic patterns as the final steady state. We attempt to understand this double possibility by using various methods, both analytical and numerical. A difficulty in this endeavour is the scarcity of hard analytical results on ''chaotic'' patterns. An early work by Newell and Pomeau [1] discussed the possibility of a chaotic ground state at threshold involving a large number of modes, named a *turbulent crystal*. They proposed a gradient system model whose ground state is

$$w(\mathbf{r}) = \frac{1}{\sqrt{N}} \sum_{j=1}^{2N} A_j \exp i\mathbf{k}_j \cdot \mathbf{r}, \tag{1}$$

where $|\mathbf{k}_j| \approx k_c$, $A_j = |A| \exp(i\phi_j)$ with independent random phases ϕ_j uniformly distributed in $\{0, 2\pi\}$. Such a structure displays chaotic behavior and short range positional order [see Fig. 1(a)]. The modes are distributed in Fourier space like the spatial spectrum of a polycrystalline sample resulting from grinding of a crystalline material into a powder, as in Fig. 1(d).

On the other hand, chaotic structures which are spatially stationary on average have been observed below the instability threshold in the presence of a continuous noise [2], or as a fluctuating ''quantum image'' [3] due to quantum noise. They are also commonly observed in numerical simulations above threshold, when starting from random initial conditions, in the linear stage before the nonlinearity comes into play and brings the system to its final state. To the best of our knowledge, no turbulent crystal has been reported as the final stage of evolution of a system without external sustained noise.

Below we study another case of two-dimensional chaotic state, the labyrinths [Fig. 1(c)], which also display short range order and a powderlike spectrum [Fig. 1(d)]. Labyrinthine structures have been observed in many situations, as in

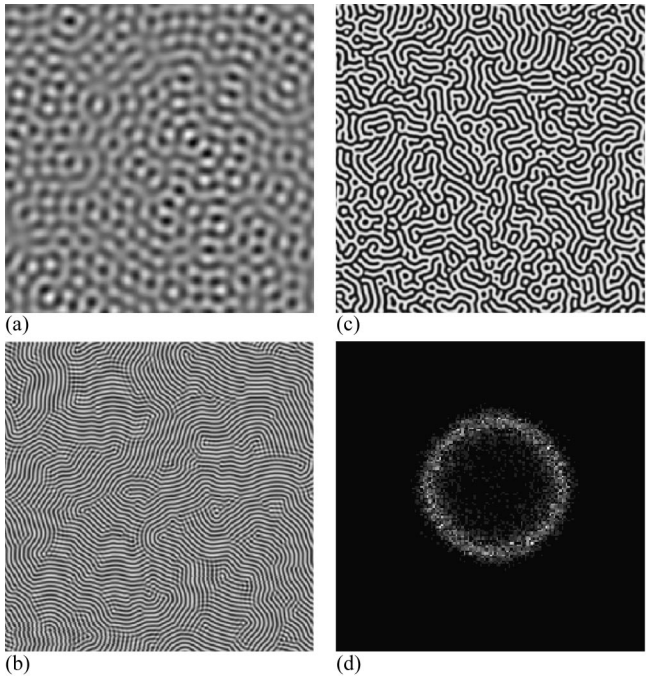

FIG. 1. (a) Newell-Pomeau turbulent crystal. (b) Domains of rolls in the transient state. (c) Stable labyrinths. (d) Spatial spectrum of (c). (b)–(d) correspond to the DOPO case, Eqs. (9) and (10), with a grid of 1024×1024 points, and 16 points per critical signal wavelength.

magnetic films [4], in chemical reactions [5], and in vibrated sand [6]. Labyrinths also appear from random initial conditions as solutions of the forced Ginzburg-Landau equation [7], of reaction-diffusion models [8], and of optical models [9,10], always without external noise. While these chaotic states are formed in many situations, no statistical approach has been proposed to account for their properties, and the bifurcation leading to labyrinths has not been considered. There is even some confusion concerning their definition, labyrinths being sometimes named rolls [11,12].

From now on the label *turbulent crystal* will be restricted to the structures predicted by Newell and Pomeau [described by Eq. (1) with large N], *labyrinths* to structures as in Fig. 1(c) already reported in the literature, and *chaotic crystals* to any structure without long range order, but spatially statistically homogeneous.

A statistical approach is first used to characterize the labyrinths, and we point out to what extent they are like or not like the Newell-Pomeau turbulent crystals. Four different model equations are considered that display similar features when starting from random initial conditions. Rolls are formed at the threshold of instability, followed by labyrinths as the control parameter increases. On the other hand, for parameter values where labyrinths appear, using parallel rolls as initial conditions, stable rolls remain forever. Our second aim is to find if a bifurcation rolls→labyrinths exists in these systems, i.e., if the labyrinth becomes the ''ground state'' above a certain threshold.

For the three variational models considered here, i.e., of type $\partial_t w = -\delta F/\delta w^*$ where w^* is the complex conjugate of w if w is complex, the ground state is the one minimizing the Euler-Lagrange functional $F(w,w^*)$, also named the ''potential'' or ''energy.'' In these cases, rolls are found to be more stable than labyrinths, the energy density of the two structures becoming closer and closer as the control parameter increases. In contrast, in the model of the degenerate optical parametric oscillator (DOPO), without variational structure, a numerical experiment shows a clear bifurcation from rolls to labyrinths as the ''preferred'' pattern.

The four model equations for our study are presented in Sec. II. In Sec. III the labyrinths are shown to be mainly described in terms of a single local wave vector. This makes them differ sharply from the Newell-Pomeau turbulent crystals involving locally an infinite number of Fourier modes. In Sec. III we compare the stability of rolls and labyrinths in the four model equations.

II. MODEL EQUATIONS

The simplest model considered here is the gradient-type Swift-Hohenberg (SH) equation for the real valued order parameter $w(r,t)$,

$$\partial_t w = \mu w - (\nabla^2 + 1)^2 w - w^3, \tag{2}$$

where $\nabla^2 = \partial_x^2 + \partial_y^2$ is the Laplacian and μ the control parameter. The zero solution destabilizes at $\mu_{\mathrm{mod}} = 0$ into a roll pattern with wave number $k = 1$. A nontrivial constant solution exists for $\mu > 1$, which is modulationally unstable for $\mu < 1.5$. The energy density for a surface Σ is

$$F\{w\} = \frac{1}{\Sigma}\int_{\Sigma} d\mathbf{r}\left[-\frac{\mu}{2}w^2 - \frac{1}{4}w^4 - \frac{1}{2}\{(\nabla^2+1)^2 w\}^2\right]. \tag{3}$$

In numerical simulations of Eq. (2), starting from random initial conditions, it seems at first that the final states exhibit a continuous transition from rolls to labyrinths as μ increases from zero. Indeed the patterns obtained at a given time have an increasing number of defects; they are composed of domains of rolls with decreasing size, which become frozen for $\mu \gtrsim 1.5$, looking like an ensemble of portions of a single curved roll or labyrinth. All these structures (either domains of rolls or labyrinths) display a powerlike spatial Fourier spectrum around the critical circle [qualitatively as in Fig. 1(d)]. The labyrinths disappear for $\mu \gtrsim 5.7$ to the benefit of the constant solution (eventually with localized structures [11]).

We have also considered two other variational models, the quintic SH equation

$$\partial_t A = \mu A - (\nabla^2 + 1)^2 A + A^3 - 0.25A^5, \tag{4}$$

chosen because of its subcritical character, and also a system of two coupled SH equations inspired by Newell and Pomeau [1],

$$\partial_t w = \mu w - (\nabla^2 + 1)^2 w - w^3 - 2r\epsilon u w - \gamma_w w^5, \tag{5}$$

$$\partial_t u = -\epsilon^2 u - (\nabla^2 + q^2)^2 u - r\epsilon w^2 - \gamma_u u^3. \tag{6}$$

Reference [1] suggests an Euler-Lagrange functional for an active mode (w), coupled to a set of passive modes (u_n), each with appropriate parameters (q_n, ϵ_n, r_n), which could lead to a ground state of a turbulent crystal with a large number of modes. We investigate a model with a single passive mode. For small values of the coupling coefficient $r\epsilon$ where a weakly nonlinear analysis has been performed, the model in Eqs. (5), (6) cannot lead to a chaotic ground state [13]. But for large coupling ($r\epsilon \gtrsim 5$), this model displays subcritical rolls and labyrinths.

Finally, we study a nonvariational model for the DOPO with the $\chi^{(2)}$ crystal filling the whole length of a ring cavity. For the values of the parameters used below, it has been shown [10,14] that diffraction and nonlinearities can be decoupled. Therefore the complex amplitudes $\alpha_{0,1}(t,\mathbf{r},z)$ of the pump and signal fields obey the following boundary conditions which couple the fields at the cell entrance ($z=0$) and exit ($z=l$):

$$\alpha_0(t+\tau,0) = \alpha_{0,\mathrm{in}} + \mathrm{Re}^{i\theta_0 + i\ell\nabla^2/2k_0}\alpha_0(t,\ell),$$

$$\alpha_1(t+\tau,0) = \mathrm{Re}^{i\theta_1 + i\ell\nabla^2 k_0}\alpha_1(t,\ell). \tag{9}$$

In Eqs. (9) the transverse $\mathbf{r}$ dependence has been dropped. τ is the round trip time of the light inside the cavity, $\alpha_{0,\mathrm{in}}$ is the input pump amplitude (taken as control parameter), ℓ is the cell length, R is the total reflectivity of

the plane mirrors, $\theta_{0,1}$ are the cavity mistunings for the two fields, and k_0 the longitudinal wave number, all real quantities. The field amplitudes $\alpha_{0,1}(t,\ell)$ at the exit of the $\chi^{(2)}$-type medium are approximated by a second order expansion:

$$\alpha_0(\ell)=\alpha_0(0)+i\ell\alpha_1^2(0)-\ell^2\alpha_0(0)|\alpha_1^2(0)|,$$

$$\alpha_1(\ell)=\alpha_1(0)+i\ell\alpha_0(0)\alpha_1^*(0) \tag{10}$$

$$+\frac{\ell^2}{2}\alpha_1(0)[|\alpha_0^2(0)|-|\alpha_1^2(0)|],$$

when the variables $(t,\mathbf{r})$ inside the parentheses are dropped. We used the parameter values $R=0.9$, $\theta_0=2\theta_1=0.2$. For $\alpha_{0,\mathrm{in}}=0.0226$ a signal field emerges with an unstable wave number k_c given by the relation $k_c^2\ell/k_0=\sqrt{\theta_1}$. With random initial conditions, when increasing the control parameter, the transverse profile of the signal field (either the real part or the imaginary part of α_1) has the same appearance as the solutions of the SH equation (2), i.e., domains of rolls are formed close to threshold [cf. Fig. 1(b) for $\alpha_{0,\mathrm{in}}=0.0245$] and then labyrinths [Fig. 1(c), $\alpha_{0,\mathrm{in}}=0.030$] until the homogeneous solution emerges ($\alpha_{0,\mathrm{in}}=0.032$).

III. STATISTICAL PROPERTIES OF LABYRINTHS

The Newell-Pomeau turbulent crystal, Fig. 1(a), clearly differs from the structures shown in Figs. 1(b)–1(c), while they all display similar spectra. As the three structures are chaotic, it is natural to use a statistical approach to help to understand the differences between them. The ensemble averages noted below by angular brackets are numerically computed by spatial averaging. We show here that labyrinths are locally periodic solutions, i.e., *textures*, in the limit of short range positional order. A texture can be written as

$$w(r)\sim\mathcal{A}\exp i\phi(\mathbf{r})+\text{c.c.}\sim\mathcal{A}\exp i\mathbf{k}(\mathbf{r})\cdot\mathbf{r}+\text{c.c.}, \tag{11}$$

with a local wave vector $\mathbf{k}(\mathbf{r})=\boldsymbol{\nabla}\phi(\mathbf{r})$, and an amplitude $\mathcal{A}$ supposed to vary slowly with respect to the phase. Many works have studied textures, since they appear preferentially to rolls in convection boxes [15]. These studies were performed under the hypothesis $\boldsymbol{\nabla}\mathbf{k}\ll k^2$, which allows derivation of an equation for the local wave vector $\mathbf{k}(\mathbf{r})$, since the behavior of $\mathbf{k}$ near singularities of the phase field [16] is algebraically slaved to the wave number k. The relative stability of these complex structures with respect to regular ones has been discussed by Cross [17].

Labyrinths can certainly not be described as roll domains with a slowly varying amplitude and orientation, because the local orientation of the nodal lines of the field changes with a typical length scale of the order of the wavelength, so that they are fundamentally disordered. However, one can define a field of wave vectors $\mathbf{k}(\mathbf{r})$ almost everywhere. To know the local orientation and magnitude of $\mathbf{k}(\mathbf{r})$, one can either draw the curves orthogonal to the nodal lines and then interpolate at each point of the grid [18,19], or use a local Fourier transform [20]. As shown below, the notion of a local wave vector describes the labyrinths well (in both variational and nonvariational systems).

In the limit of $N\to\infty$, the Newell-Pomeau field with N independent modes is Gaussian, since the random function $w(\mathbf{r})$ in Eq. (1) is the sum of a large number of independent contributions. In their original model Newell and Pomeau assumed equal amplitudes $|A_j|=|A|$ and equal wave numbers $k_j=k_c$, but a *generalized* Newell-Pomeau crystal with independent random amplitudes $|A_j|$ and random wave numbers k_j distributed around k_c is also Gaussian. In $\mathbf{r}$ space, a Gaussian crystal looks like a sort of modulated labyrinth [Fig. 1(a)] (to the eye the appearance is actually independent of the statistics of the $|A_j|$ as soon as $N\gtrsim 20$). For the Gaussian case the one-point moments $M_{2n}=\langle w^{2n}(\mathbf{r})\rangle/\sigma^{2n}$, where $\sigma^2=\langle w^2(\mathbf{r})\rangle=(1/2N)\Sigma_j^{2N}|A_j^2|$, are given by the relations

$$M_{2n,g}=(2n-1)!!, \tag{12}$$

where $(2n-1)!!=(2n)!/(2^n n!)$.

The moments for a texture are noticeably different. Using Eq. (11), and assuming $\mathcal{A}=|\mathcal{A}|e^{i\phi_0}$, where the random phase ϕ_0 is supposed to be uniformly distributed in $[0,2\pi]$ in order to ensure the spatial stationarity of the pattern, the binomial relation

$$w(\mathbf{r})^{2n}=|\mathcal{A}^{2n}|\sum_{p=1,n}C_p^{2n}e^{i(2n-2p)[\phi(\mathbf{r})+\phi_0]}$$

leads to

$$M_{2n}=\frac{(2n-1)!!}{n!}, \tag{13}$$

which is considerably smaller than the Gaussian moments, as reported on a logarithmic scale in Fig. 2(a).

The relation (13) neglects the effects of harmonics and defects of the texture. When the harmonics become important, the structures get stiff walls. In the limit of square waves, $w(\mathbf{r})=\pm w_{\max}$, then $M_{2n,\mathrm{stiff}}=1$, as for the flat solution.

Numerically, the n dependence of M_{2n} for labyrinths and domains of rolls in the SH or DOPO model [Fig. 2(a)] is close to Eq. (13). Very close to the modulational instability threshold $\alpha_{\mathrm{in,mod}}$ the moments for domains of rolls (crosses) are slightly larger than the pure $\cos[\phi(\mathbf{r})+\phi_0]$ case, Eq. (13), probably due to the presence of many defects in our transient pattern obtained in a very large aspect ratio system. As the control parameter is increased, the moments (full circles) decrease below the pure $\cos[\phi(\mathbf{r})+\phi_0]$ case, a signature of the increasing nonlinearities. The discrepancy between the moments for labyrinth and relation (13) increases with n. However in the case of the quintic SH equation (4), high order moments agree well with Eq. (13). Therefore our results point to a small effect of disclinations, or superposition of rolls with different orientations.

The probability distribution can be derived from the moments appearing in the expansion of the characteristic function

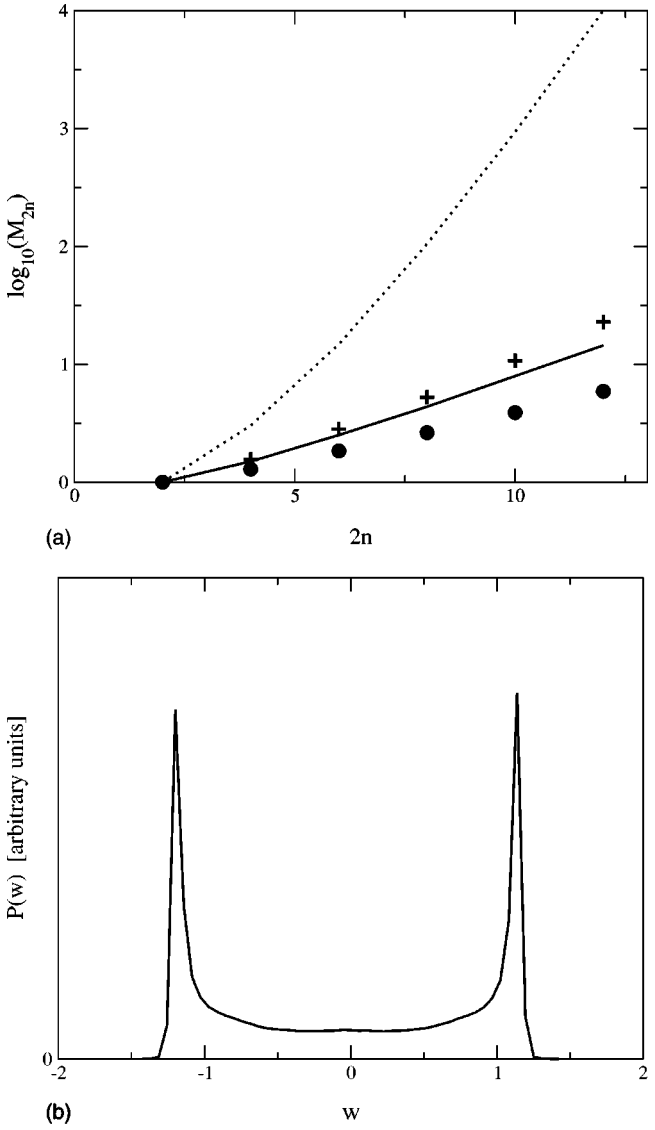

FIG. 2. (a) Moments M_{2n}, as a function of $2n$. Dotted line for the Gaussian case [Eq. (12)], solid line for Eq. (13), crosses for Fig. 1(b), circles for Fig. 1(c). (b) Probability distribution of the real part of the signal field α_1 for Fig. 1(c).

$$\Phi_w(u)=\langle e^{iuw}\rangle=\sum\ (-u\sigma)^{2n}M_{2n}\frac{1}{(2n)!}. \qquad (14)$$

$\Phi_w(u)=J_0(u\sigma/\sqrt{2})$, where J_0 is the zero-order Bessel function; the probability distribution is the Fourier transform of the probability distribution

$$p_w(w)\propto(w_{\max}^2-w^2)^{-1/2}, \qquad (15)$$

with $p_w(w)=0$ for $|w|>w_{\max}$, i.e., a U curve as shown for the labyrinth case in Fig. 2(b). The relation (15) may also be obtained directly from Eq. (11), since $p_w(w)$ is the probability distribution of the variable $w=\cos y$ where y is uniform in the range $[0, 2\pi]$.

Let us now consider the two-point moments, i.e., the correlation function and the spatial spectrum of $w(\mathbf{r})$ which gives information about the spatial correlation effects. As

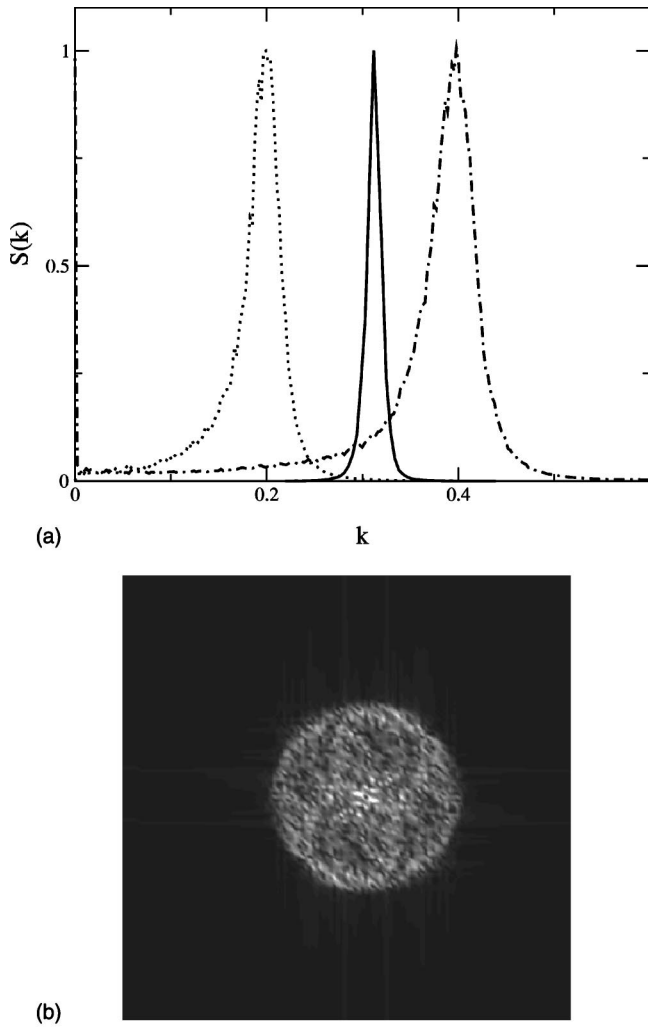

FIG. 3. (a) Structure factor for the DOPO case; left and right correspond to α_1 and α_1^2, respectively, of Fig. 1(c), and center to Fig. 1(b). The k shift between the two left curves is a consequence of the ''nonlinear resonance effect'' [25]. (b) Spatial spectrum w^2 for a generalized Newell-Pomeau turbulent crystal having the same structure factor $S_{\rm lab}(k)$ as the labyrinth in Fig. 1(c) ($N=800, |A_j|=\sqrt{S_{\rm lab}(k_j)}$ and independent random phase ϕ_j.

written above the spatial spectrum $\gamma_w(\mathbf{k})$ of generalized Newell-Pomeau turbulent crystals and of textures (with average domain size much smaller than the system size) displays no preferred direction since it appears like a powder sprinkled around a ring of radius k_c, as illustrated in Fig. 1(d) for labyrinths. The circular average of $\gamma_w(\mathbf{k})$ over $\mathbf{k}$ orientations provides a structure factor $S_w(k)$, whose width is inversely proportional to the average domain size in the case of a texture. As shown in Fig. 3(a), the structure factor of labyrinths exhibits a thick peak (dotted line), and a long tail toward small wave numbers, different from the case of domains of stripes (solid line). Therefore the shape of the structure factor reflects the appearance of a texture. Surprisingly, Gaussian crystals look the same whatever the width of the structure factor is.

The correlation function $\Gamma_w(\mathbf{r}+\mathbf{r}',\mathbf{r}')=\langle w(\mathbf{r}+\mathbf{r}')w(\mathbf{r}')\rangle$ depends on $r=|\mathbf{r}|$ for a stationary random func-

tion with rotational symmetry. In the case of textures composed of many small size domains, Eq. (11) leads to

$$\Gamma_w(r) = \langle w(\mathbf{r}) w(\mathbf{0}) \rangle = |\mathcal{A}^2| \{ \langle \exp[i\mathbf{k}(\mathbf{r}) \cdot \mathbf{r}] \rangle + \text{c.c.} \}. \quad (16)$$

With $\mathbf{k} = (k, \theta_k)$ and $\mathbf{r} = (r, \theta_r)$, Eq. (16) becomes

$$\Gamma_w(r) = \frac{|\mathcal{A}^2|}{2\pi} \int \int dk\, d\theta_k k \times \exp[ikr \cos(\theta_k - \theta_r) p(k, \theta_k)] + \text{c.c.}$$

or

$$\Gamma_w(r) \propto \int dk\, k J_0(kr) S_w(k), \quad (17)$$

assuming that the probability distribution of $\mathbf{k}$ is $p(k, \theta_k) \propto S_w(k)$. Note that Eq. (17) is also valid for a Gaussian crystal since Eq. (1) leads to $\langle w(\mathbf{r}) w(\mathbf{0}) \rangle = \lim_{N \to \infty} (1/2N) \Sigma \langle |A_j|^2 \exp(i\mathbf{k}_j \cdot \mathbf{r}) \rangle$.

The circularly averaged correlation functions of the patterns shown in Figs. 1(b) and 1(c) are drawn in Fig. 4(a). The role of the finite width of the structure factor is to change the long range behavior of $\Gamma_w(r)$. For a Dirac-like structure factor, the oscillations of $\Gamma_w(r) = J_0(kr)$ are slowly damped over several correlation lengths, the successive maxima decreasing as $\Gamma_{\max}(r) \sim r^{-1/2}$. This is illustrated in the top curve of Fig. 4(b). In contrast, in the case of a finite width structure factor, the successive maxima decrease faster. For example, when the structure factor is a meromorphic function with poles in the complex plane, the residue theorem leads to an exponential decrease of the maxima [21], as observed in Fig. 4(b) for domains of rolls and labyrinths.

The difference between labyrinths and turbulent crystals appears through the higher order momenta. For the Gaussian case

$$\Gamma_{w_p^2}(r) = \langle w_g^2(\mathbf{r} + \mathbf{r}') w_g^2(\mathbf{r}') \rangle = 2\Gamma_{w_g}^2(r) + \sigma^4, \quad (18)$$

whose Fourier transform is $\gamma_{w^2}(\mathbf{k}) = 2\gamma_w(\mathbf{k}) * \gamma_w(\mathbf{k}) + \sigma^4 \delta(\mathbf{k})$, where $*$ stands for convolution. Therefore the spatial spectrum of w_g^2 contains components *in the whole disk* with radius smaller than $2k_c$, as illustrated in Fig. 3(b). In contrast, for a texture, Eq. (9) leads to

$$\Gamma_{w^2}(r) = \{ |\mathcal{A}|^4 \langle \exp[2i\mathbf{k}(\mathbf{r}) \cdot \mathbf{r}] \rangle + \text{c.c.} \} + \sigma^4, \quad (19)$$

where $\langle \exp[2i\mathbf{k}(\mathbf{r}) \cdot \mathbf{r}] \rangle \propto \int dk\, J_0(kr) k S_w(k/2)$. Then the spatial spectrum of w^2 contains a bright spot in the center, and a powderlike ring of radius $2k_c$, as observed for labyrinths [Fig. 3(a), right curve].

The moments $\langle w(\mathbf{r} + \mathbf{r}') w^3(\mathbf{r}') \rangle$ also differ. For the Gaussian case, $\langle w_g(\mathbf{r} + \mathbf{r}') w_g^3(\mathbf{r}') \rangle = 3\sigma^2 \Gamma_{w_g}(\mathbf{r})$, while for a labyrinth the numerical data exactly fit the relation

$$\langle w(\mathbf{r} + \mathbf{r}') w^3(\mathbf{r}') \rangle = \frac{3}{2} \sigma^2 \Gamma_w(\mathbf{r}), \quad (20)$$

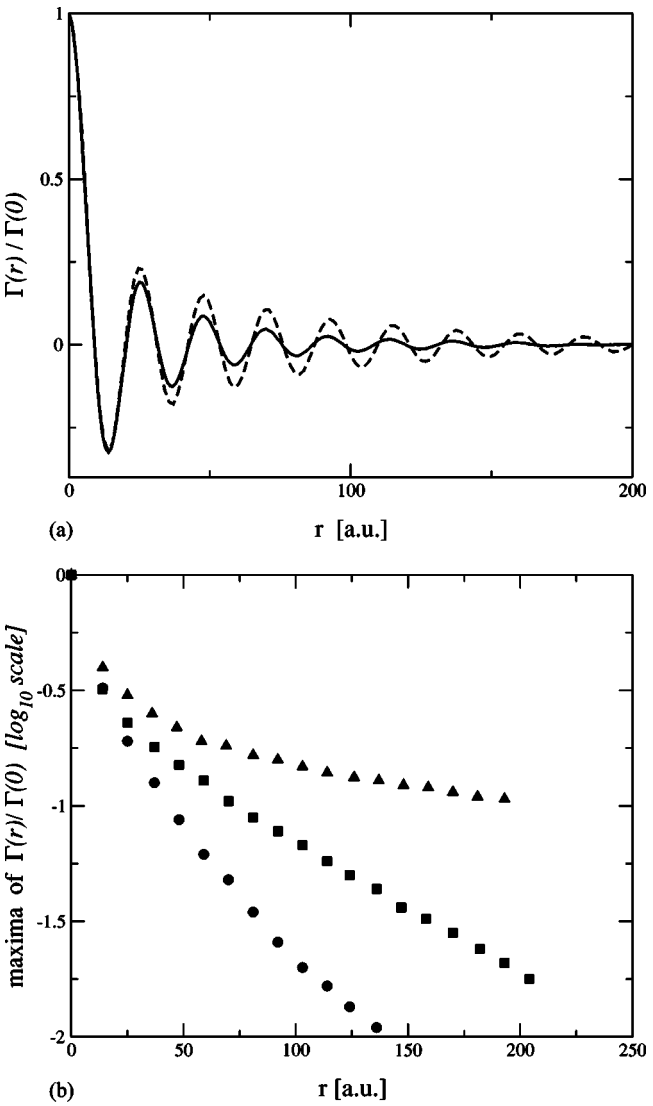

FIG. 4. Circularly averaged correlation function for Figs. 1(b) and 1(c) of the DOPO; r is scaled in order that the maxima coincide. (a) $\Gamma(r)/\Gamma(0)$ for the labyrinths (solid line) and domains of rolls (dashed line). (b) Height of the successive maxima: top curve for $J_0(r)$, middle curve for domains of rolls, and bottom curve for labyrinths.

which agrees with a texture description, Eq. (11).

We have shown that a local wave vector can be defined almost everywhere for a labyrinth. Therefore a labyrinth can be described as a texture, but in the short range order limit, since the orientation of the local wave vector changes over a distance as short as the spatial period. Although labyrinths differ markedly from Newell-Pomeau crystals in which an infinite number of wave vectors contributes to the structure at each point $\mathbf{r}$, they are chaotic crystals as well as the Gaussian crystals, in the sense that the two structures have small coherence length and a powderlike spectrum.

IV. TRANSITION FROM ROLLS TO LABYRINTHS

In the preceding section we have examined the properties of chaotic structures, labyrinths, that are both homogeneous

on average and random at short scale. They are found as the final state of the evolution of equations like the SH and DOPO equations. The same equations for the same parameter values also have a periodic roll solution as the final state. This shows that the final state depends on the initial conditions. In thermodynamics, for the same range of parameters (temperature, for instance) one may observe a thermodynamically stable and a metastable state. Here, to decide which is which, we took inspiration from thermodynamics where unless special conditions are met, the ''stable'' state tends to invade the ''metastable'' one. We have tried to do the same in our models, with the help of a numerical test. The results are reported below.

The numerical test was first probed on the SH variational model where the relative stability of the solutions is known from the calculation of energy density (per unit area) F. In Fig. 5(a) the energy density F_{roll} of the parallel roll pattern is drawn versus the wave number, and compared with the energy density F_{lab} of various labyrinthine patterns obtained from different initial conditions [22]. The roll pattern with optimal wave number is shown [Fig. 5(b)] to be more stable than the labyrinth in the whole domain where the latter exists. In this range the energy for rolls is 4–10 % lower than for labyrinths. Labyrinths disappear at $\mu=5.7$ where the homogeneous state becomes more stable than rolls.

It would be interesting to know if this property (lower energy for rolls than for labyrinths) is just an accident of this model, or due to the fact that we are looking at two dimensions, etc. Therefore we have also compared the energy densities for two other variational models, Eqs. (4) and (5), (6).

For Eq. (4), similar results (not reported here) are obtained with the added complexity of an unstable constant solution.

In the case of Eqs. (5), (6), again parallel rolls are more stable than labyrinths. For $r\varepsilon\geqslant 7$, and $\mu\approx 0.1$ the energy difference between them may be as small as 3%, which is larger than the fluctuations of the final values of F_{lab} when changing the initial conditions (they are smaller than 1%).

The numerical test that was first used [24] to decide which structure (rolls or labyrinths) is the preferred state was the following: We looked at the evolution of an initial pattern filled with stripes on one half, and with a labyrinth on the other half. For Eqs. (2), (4), (5), and (6) the rolls (more stable than labyrinths as stated above) partially invade the labyrinth part. But this test may be biased due to the periodic boundary conditions. For example, when the grid size is exactly equal to an integer number of wavelengths, the roll component is essentially frozen. In order to get rid of the boundary problem, we present here another numerical test: We look at the evolution of a droplet of rolls inside a labyrinthine sea.

For the SH model, the droplet grows, Figs. 6(a) and 6(b). The evolution was quantified by a study of the temporal evolution of the angular distribution of the spatial spectrum $S(\vartheta_{\mathbf{k}})=\int dk|w(k,\vartheta_{\mathbf{k}})|^2$ drawn in Fig. 7(a). The area occuped by parallel rolls is proportional to $S_{\max}(\vartheta_{\mathbf{k}})$ which increases and then oscillates as shown in the upper curve of Fig. 7(b).

For the DOPO case, Eqs. (9), (10), which has no obvious formulation in terms of a relaxing functional for the parameter values we consider here [23], the droplet also expands close to the threshold, but it shrinks for $\alpha_{0,\mathrm{in}}\geqslant\alpha_{0,\mathrm{lab}}$ as shown in Figs. 6(c) and 6(d). In the latter case the quantity $S_{\max}(\vartheta_{\mathbf{k}})$ decreases and then oscillates as shown in the lower curve of Fig. 7(b). Consequently, in the DOPO system, there is evidence of a transition from rolls to labyrinths as the more stable final state. When $\alpha_{0,\mathrm{in}}$ is increased further, the labyrinth destabilizes into a flat planform, as in the SH case.

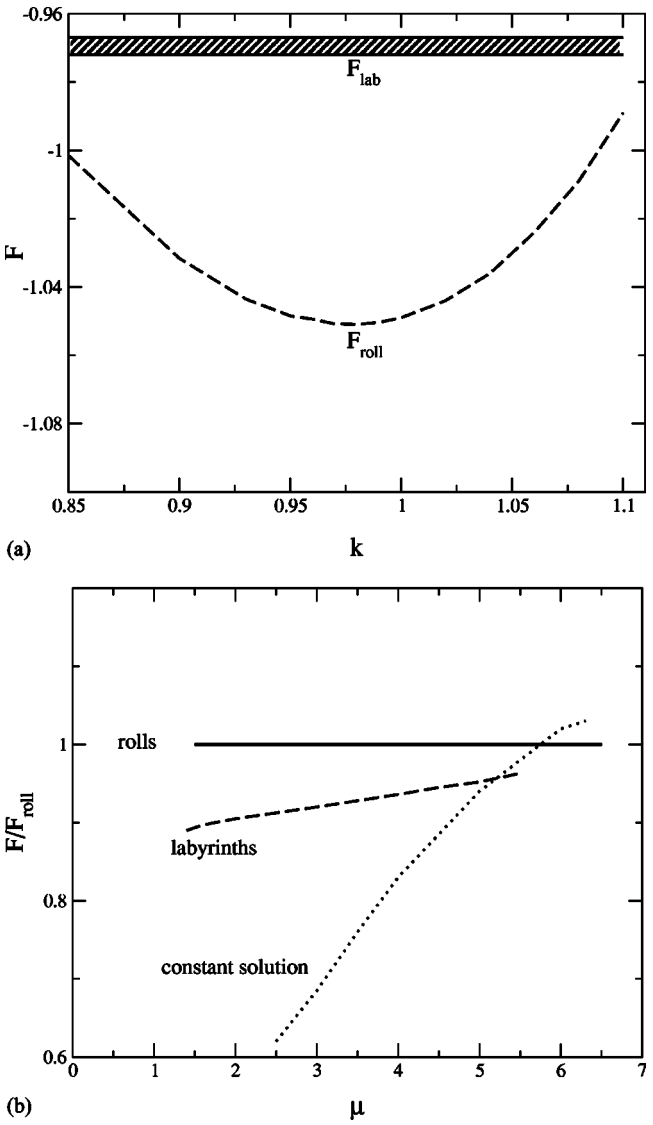

FIG. 5. Comparison of the energy density F for parallel rolls and labyrinths. (a) $F(k)$ for Eqs. (5), (6), $\epsilon r=5$, $\mu=0.1$, $q^2=1.5$. (b) Energy $F/F_{\mathrm{rolls}}(\mu)$ for parallel rolls (with optimal wave vector), labyrinths, and constant solution for Eq. (2). The more stable state corresponds to the upper curve, because $F<0$.

V. CONCLUSION

Up to now a Newell-Pomeau turbulent crystal defined by Eq. (1), as a linear superposition of many Fourier modes, has never been observed as a stable two-dimensional pattern, without sustained external noise. Seemingly such a structure can hardly survive the nonlinear selection stage at least in

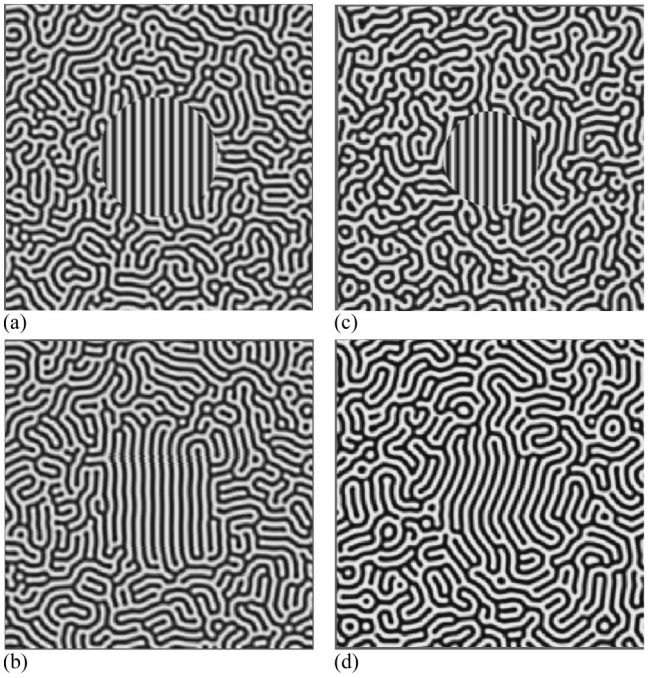

FIG. 6. Evolution of a droplet of rolls inside a labyrinthine sea. (a), (b) Patterns at $t=0$ and 0.9×10^5 for the SH Eq. (2), $\mu=1.6$, with a 256×256 grid, and eight points per wavelength. (c), (d) Patterns at $t=0$ and 2×10^5 in units of the cavity photon lifetime $\tau/(1-R)$ for the DOPO case, $\alpha_{0,\mathrm{in}}=0.030$, with a 512×512 grid, and 16 points per signal wavelength (eight points for the pump field).

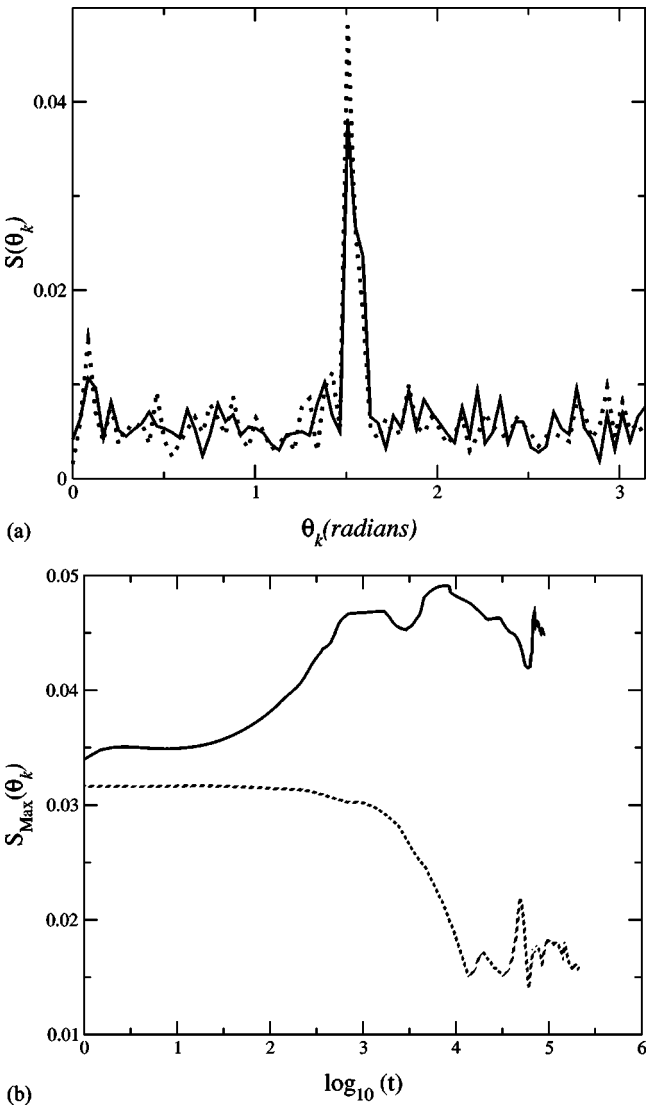

FIG. 7. (a) Angular distribution of the spatial spectrum for the patterns of Figs. 6(a) (dotted line) and 6(b) (solid line). (b) Time evolution of $S_{\max}(\vartheta_{\mathbf{k}})$ for the patterns of Figs. 6(a)–6(d); upper curve for the SH equation and lower curve for the DOPO case beyond the bifurcation to labyrinths.

low space dimension. In this paper we have analyzed two kinds of chaotic structure with short range positional order and a powderlike spatial spectrum, the turbulent crystal and the labyrinth. For labyrinths, unlike the turbulent crystal, a single wave vector may be defined locally almost everywhere. Thus a labyrinth is a limit case of a texture with a coherence length comparable to the wavelength.

In the various models studied here, although the evolution of the pattern looks the same, a bifurcation from rolls to labyrinths is clearly shown in the DOPO model only, where a droplet of rolls first expands and then shrinks at increasing values of the control parameter. In contrast, in the three variational models, rolls are more stable than labyrinths whatever the control parameter might be. However, even very close to the threshold, domains of rolls do not evolve toward parallel rolls, as recently shown [26], due to the pinning of the grain boundaries in an effective periodic potential induced by the periodicity of the stripe pattern itself.

The general question of the spatial structure of ground states of given systems does not yet have a well understood answer. Our numerical studies seem to exclude the possibility of chaotic ground states for the simple variational models we looked at, although the energy difference between the labyrinthine state and the rolls may be quite small. But other gradient models may well have chaotic ground states. From the point of view of order in crystals, Landau proposed long ago considering crystals as generated by coupled density waves, which is theoretically close to the kind of models we look at. This idea of a ground state described by weakly interacting modulation waves is believed to be a fair approximation for some liquid crystals, for instance. At the moment we are actively looking at the possibility of chaotic ground state in space dimension 3 where the simple approach of Newell-Pomeau does not apply (the unit sphere in the momentum space cannot be tiled uniformly with regular polyhedra with an arbitrarily large number of vertices).

ACKNOWLEDGMENTS

The numerical work was done at the computer center of the CNRS (IDRIS) and at the computer center of Paris-Sud University (CRI). We thank IDRIS and CRI for their help. Paul Manneville is warmly thanked for very helpful discussions.

[1] A. C. Newell and Y. Pomeau, J. Phys. A **26**, L429 (1993).
[2] C. Szwaj (private communication); see also M. Wu, G. Ahlers, and D. S. Cannell, Phys. Rev. Lett. **75**, 1743 (1995).
[3] A. Gatti, H. Wiedemann, L. A. Lugiato, I. Marzoli, G. L. Oppo, and S. M. Barnett, Phys. Rev. A **56**, 877 (1997).
[4] A. H. Bobeck, Bell Syst. Tech. J. **46**, 1901 (1967); R. E. Rosensweig, Sci. Am. **247**, 135 (1982); see also *Magnétisme, Tome 1: Les Fondements* (University of Grenoble Press, Grenoble, 2001).
[5] Kyoug J. Lee, W. D. McCormick, Qi Ouyang, and H. L. Swinney, Science **261**, 192 (1993).
[6] D. H. Rothman, Phys. Rev. E **57**, R1239 (1998).
[7] P. Coullet and K. Emilsson, Physica D **61**, 119 (1992).
[8] S. Metens, Ph.D thesis, University of Brussels, Belgium, 1998.
[9] R. Gallego, M. San Miguel, and R. Toral, Phys. Rev. E **61**, 2241 (2000).
[10] M. Le Berre, E. Ressayre, and A. Tallet, J. Opt. B: Quantum Semiclassical Opt. **2**, 347 (2000).
[11] K. Ouchi and H. Fujisaka, Phys. Rev. E **54**, 3895 (1996).
[12] Q. Ouyang and H. L. Swinney, Chaos **1**, 411 (1991).
[13] In Eqs. (5) and (6), the damping coefficients $\gamma_{w,u}$ have been introduced to prevent divergence of the solutions. A weakly nonlinear analysis was performed for $\gamma_w=\gamma_u=0$, by using the expansion (1) with $|k_j|=1$ for w, and a similar expansion for u (with wave numbers varying between 0 and 2, due to the quadratic coupling). Using the same notation as in Refs. [1], [18] the coupling coefficient between the two active and passive modes is

$$\beta(\theta)=6-4r^2\{L(q^2)+L(q^2-K_-^2)+L(q^2-K_+^2)\}, \qquad (7)$$

where $L(q^2)$ is the Lorentzian $\varepsilon^2/(\varepsilon^2+q^4)$ and $k_\pm^2=2(1\pm\cos\theta)$, and the self-interaction coefficient is

$$\beta_0=3\{1-2r^2L(q^2)\}. \qquad (8)$$

The condition required [1] for a turbulent crystal [i.e., that the coupling function $\beta(\theta)$ is flat and very small in the whole domain $(0,\pi)$] is fulfilled only for $q^2\simeq 0$, very small ε^2 and r^2 close to 3/2; but this case leads to a negative β_0. A positive β_0 is reachable only for peaked (nonflat) $\beta(\theta)$, so that it would lead to the usual N-gon structures, with $N=1$, 2, 3.
[14] The model in Eqs. (9) and (10) gives comparable results with the mean-field model introduced by G. L. Oppo, M. Brambilla, and L. Lugiato, Phys. Rev. A **49**, 2028 (1994) for small values of $\alpha_{0,1}\ell$, as shown by M. Tlidi, M. Le Berre, E. Ressayre, A. Tallet, and L. Di Menza, *ibid.* **61**, 043806 (2000).
[15] M. C. Cross and A. C. Newell, Physica D **10**, 299 (1984).
[16] A. C. Newell, T. Passot, C. Bowman, N. Ercolani, and R. Indik, Physica D **97**, 185 (1996).
[17] M. C. Cross, Phys. Rev. A **25**, 1065 (1982).
[18] P. Manneville, *Structures Dissipatives Chaos et Turbulene* (Aléa, Saclay, France, 1990).
[19] M. S. Heutmaker, P. N. Fraenkel, and J. P. Gollub, Phys. Rev. Lett. **54**, 1369 (1985).
[20] C. Bowman and A. C. Newell, Rev. Mod. Phys. **70**, 289 (1998).
[21] For nonanalytic functions, or for analytic functions $kS(k)$ without any pole in the complex k plane, the result could be different. For example, in the case of a square shaped structure factor $S(k)=1$ for $k_c-\delta k\leqslant k\leqslant k_c+\delta k$, the asymptotic behavior $J_0(k_cr)\sim(1/\sqrt{kr})\cos(kr-\pi/4)$ leads to the power law behavior $\Gamma_{\max}(r)\sim r^{-3/2}$.
[22] This procedure was implemented by P. Manneville in the case of the SH equation (private communication).
[23] A weakly nonlinear analysis proves that the mean-field model, and therefore also Eqs. (9) and (10), reduce to the SH equation (2), in the limit of small negative mistunings [25] $\Delta_{0,1}=-\theta_{0,1}/(1-R)\to 0$. But our study of the DOPO concerns the case $\Delta_0=2\Delta_1=-2$, outside the validity range of the approximation of a DOPO by the SH equation.
[24] L. Di Menza, M. Le Berre, Y. Pomeau, E. Ressayre, and A. Tallet, *Rencontre du Non-Linéaire* (IHP, Paris, 2001).
[25] G. J. de Valcarcel, K. Staliunas, E. Roldan, and V. J. Sanchez-Morcillo, Phys. Rev. A **54**, 1609 (1996).
[26] D. Boyer and J. Vinals, Phys. Rev. E **64**, 050101 (2001); **65**, 046119 (2002).